Journal of Sound and Vibration (1998) **213**(1), 15–33

FREE VIBRATION ANALYSIS OF SHELLS OF REVOLUTION

D.-Y. TAN

School of Civil Engineering, The University of Birmingham, Edgbaston, Birmingham B15 2TT, England

(*Received* 25 *June* 1997, *and in final form* 31 *October* 1997)

An efficient substructuring analysis method is presented for predicting the natural frequencies of shells of revolution which may have arbitrary shape of meridian, general type of material property and any kind of boundary condition. This method is developed in the context of first order shear deformation shell theory as well as the classical thin shell theory. The vibrational behaviours of a circular cylinder, an elliptic hyperboloid shell (modelling a cooling tower) and a complete spherical shell are investigated using this method.

1. INTRODUCTION

As shell structures have comparatively light weight and high load capacity and are able to provide a big span of space, they have been widely used in aerospace engineering, marine engineering, power plant engineering and civil engineering. The understanding of their mechanical behaviour under static, dynamic and thermal loads is of considerable importance. Although the history of the investigations into the mechanical behaviour of shell structures can be traced back to about a century ago, finding a satisfactory solution for a general shell structure with any kind of boundary specification is still a big challenge both analytically and numerically [1, 2].

A shell of revolution is a special type of shell structure which is axi-symmetric. This paper proposes a numerical method in the context of both the first order shear deformation shell theory (SDST) and the classical thin shell theory (TST) for analyzing the vibrational behaviour of a shell of revolution which may have an arbitrarily shaped meridian, general type of material property and any kind of boundary condition. This method is very efficient because it effectively uses the symmetry property of a shell of revolution. The shell of revolution is discretized by the meridians circumferentially, and general spline functions and Lagrangian polynomials are used to represent the displacement variations along the meridian and in the circumferential direction in an element, respectively. So the shape function of an element is a mix of a spline family and a Lagrangian polynomial family. As higher degree of spline functions and higher order of Lagrangian polynomials are used for an element, the higher order of displacement continuity is preserved. In finding the natural frequencies of a shell of revolution, the Sturm sequence method [3, 4] is used in conjunction with the massive substructuring technique. The vibrational behaviour of a circular cylinder, an elliptic hyperboloid shell and a spherical shell are investigated with respect to the different kinds of material property that they have.

0022–460X/98/210015 + 19 $25.00/0/sv971406

2. DISPLACEMENT REPRESENTATION OF AN ELEMENT

2.1. GEOMETRY DESCRIPTION OF AN ELEMENT

Figure 1 shows a basic element of a shell of revolution which may, in general, be a laminate having arbitrary lay-up of a number of layers of fibre-reinforced composite material. In the element, the natural co-ordinates are used. For a shell of revolution, this natural co-ordinate system is orthogonal and happens to be the lines of curvature.

According to the first order shear deformation shell theory [5, 6], the behaviour of the shell is characterized by the five fundamental displacement-type quantities indicated in Figure 1, namely u, v and w, the translational displacements at the middle surface in the s, t and z directions, respectively, and ψ_s and ψ_t, the rotations of the middle surface normal along the s and t directions, respectively. However, in the classical thin shell theory the Kirchhoff normal rotation condition is invoked and the rotation ψ_s and ψ_t are directly related to the deflection w and displacements u and v by the way of equations:

$$\psi_s = u/R_s - \partial w/\partial s, \qquad \psi_t = v/R_t - \partial w/\partial t. \tag{1}$$

It follows, of course, that shell behaviour in TST analysis can be represented by three fundamental quantities, namely u, v and w, rather than the five fundamental quantities of SDST analysis.

In the present approach, the physical displacements are only specified at some locations on several so called reference meridians. The displacements elsewhere in the element are interpolated from them. On the reference meridians, spline interpolation is used. Between the reference meridians, polynomial interpolation is used.

2.2. DISPLACEMENT REPRESENTATION ALONG THE MERIDIAN

Let $b^i_{m,n}(s)$ be the basis spline function of degree m defined on the ith reference meridian with the knot sequence $(s^i_n)_{n\in\mathscr{Z}}$ ($\mathscr{Z}$ is the set of integer numbers). It can be proved that the basis spline function is unique and can be expressed as a linear combination of the so-called truncated power functions which are typical cardinal spline functions, i.e., [7]

$$b^i_{m,n}(s) = \sum_{0 \leqslant k \leqslant m+1} a^i_{k,n} (s - s^i_{n+k})^m_+, \tag{2}$$

where $(s - s^i_{n+k})_+ = \sup(s - s^i_{n+k}, 0)$, and the real coefficients $a_{k,n}$ satisfy the following equations [7]:

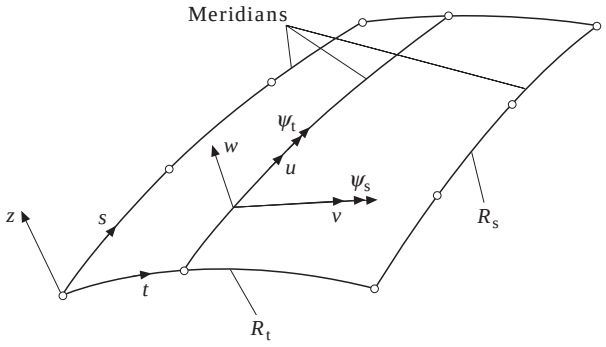

Figure 1. An element.

$$\sum_{0 \leqslant k \leqslant m+1} a^i_{k,n} (s^i_l - s^i_{n+k})^m = 0, \qquad (l = n+1, \ldots, n+m+1), \tag{3}$$

$$\sum_{0 \leqslant k \leqslant m+1} a^i_{k,n} (s^i_{n+m+1} - s^i_{n+k})^{m+1} = m+1. \tag{4}$$

Let $f(s, t)$ be a continuous function, for example it may be $u(s, t)$, $v(s, t)$, $w(s, t)$, $\psi_s(s, t)$ or $\psi_t(s, t)$. When t is constrained on the ith reference meridian, i.e., $t = t_i(s)$, $f(s, t_i(s))$ becomes a continuous function on it. So, $f(s, t_i(s))$ can be approximated by the spline interpolation as follows,

$$f(s, t_i(s)) = \sum_{n=1}^{N^i_s} \alpha_{n,i} b^i_{m,n}(s), \tag{5}$$

where $\alpha_{n,i}$ are interpolation coefficients which should be determined by the specified conditions of $f(s, t_i(s))$ on the reference meridian, and N^i_s is the total number of basis splines used for the ith meridian. The specified conditions of $f(s, t_i(s))$ are chosen to be:

$$\begin{aligned}\mathbf{f}_i = [&f(s_1, t_i(s_1)), \quad f^{(1)}(s_1, t_i(s_1)), \ldots, f^{(m_l)}(s_1, t_i(s_1)), \quad f(s_2, t_i(s_2)), \quad f(s_3, t_i(s_3)), \ldots, \\ &f(s_{N^i_s - m}, t_i(s_{N^i_s - m})), \quad f^{(1)}(s_{N^i_s - m}, t_i(s_{N^i_s - m})), \ldots, f^{(m_r)}(s_{N^i_s - m}, t_i(s_{N^i_s - m}))]^{\mathrm{T}},\end{aligned} \tag{6}$$

where $m_l = m/2 - \mathrm{mod}(m, 2)$, $m_r = m - m_l - 1$.

Substituting these specified conditions in equation (5), the obtained $\alpha_{n,i}$ are,

$$\alpha_i = \mathbf{R}_i^{-1} \mathbf{f}_i, \tag{7}$$

where the elements of $\mathbf{R}_i$ are,

$$\mathbf{R}_i(l, k) = \begin{cases} b^{i(n)}_{m,k}(s_1) & (l = n+1; n = 0, 1, \ldots, m_l; \quad k = 1, 2, \ldots, N^i_s) \\ b^i_{m,k}(s_n) & (l = m_l + n; n = 2, 3, \ldots, N^i_s - m; k = 1, 2, \ldots, N^i_s), \\ b^{i(n)}_{m,k}(s_{N^i_s - m + 1}) & (l = N^i_s - m_r + n; n = 0, 1, \ldots, m_r; k = 1, 2, \ldots, N^i_s) \end{cases} \tag{8}$$

and $\alpha_i = [\alpha_{1,i}, \alpha_{2,i}, \ldots, \alpha_{N^i_s, i}]^{\mathrm{T}}$.

Combining equations (5) and (7), the spline interpolation of $f(s, t_i(s))$ with its specified values is,

$$f(s, t_i(s)) = \mathbf{B}^i_m(s) \mathbf{f}_i, \tag{9}$$

where

$$\mathbf{B}^i_m(s) = [b^i_{m,1}(s), b^i_{m,2}(s), \ldots, b^i_{m,N^i_s}(s)] \mathbf{R}_i^{-1}. \tag{10}$$

2.3. DISPLACEMENT REPRESENTATION IN THE CIRCUMFERENTIAL DIRECTION IN SDST

When s is fixed, $f(s, t)$ becomes a continuous function in the circumferential t-direction whose values are restricted to $f(s, t_i(s))$ on its junctions with the reference meridians. As only C^0-type continuity is required on the displacements in SDST, the Lagrangian polynomial interpolation could be used in this direction. Therefore, $f(s, t)$ can be approximated as,

$$f(s, t) = \sum_{i=1}^{i_p} P_i(t, s) f(s, t_i(s)), \tag{11}$$

where $P_i(t, s)$ $(i = 1, 2, \ldots, i_p)$ are Lagrangian polynomial functions, for instance when $i_p = 4$, they are,

$$P_1(\eta) = (-1 + \eta + 9\eta^2 - 9\eta^3)/16, \qquad P_2(\eta) = (9 - 27\eta - 9\eta^2 + 27\eta^3)/16,$$
$$P_3(\eta) = (9 + 27\eta - 9\eta^2 - 27\eta^3)/16, \qquad P_4(\eta) = (-1 - \eta + 9\eta^2 + 9\eta^3)/16, \tag{12}$$

where $\eta = 2t/b(s)$, and $b(s)$ is the circumferential arc length of the element at the position s on the meridian.

2.4. DISPLACEMENT REPRESENTATION IN THE CIRCUMFERENTIAL DIRECTION IN TST

In classical thin shell theory, the continuity requirement on displacements $u(s, t)$ and $v(s, t)$ is the same as that in SDST. So, they can be approximated in the same way as before using equation (11). However, as the Kirchhoff condition expressed by equation (1) the requirement of the C^1-type continuity of $w(s, t)$ is necessary. That means the first derivatives of $w(s, t)$ in the circumferential direction (i.e., $\partial w/\partial t$) should be used as freedoms at the outside meridians of the element. This condition limits the choice for the interpolation function for $w(s, t)$ in the circumferential direction. When $i_p = 4$, Hermitian functions satisfy this condition. They are,

$$P_{1H}(\eta) = (2 - 3\eta + \eta^3)/4, \qquad P_{2H}(\eta) = b(1 - \eta - \eta^2 + \eta^3)/8,$$
$$P_{3H}(\eta) = (2 + 3\eta - \eta^3)/4, \qquad P_{4H}(\eta) = b(-1 - \eta + \eta^2 + \eta^3)/8, \tag{13}$$

where $\eta = 2t/b(s)$. In this case, the approximation of $w(s, t)$ can be expressed as,

$$w(s, t) = \sum_{i=1}^{4} P_{iH}(t, s)\mathbf{B}^i_{m_3}(s)\mathbf{w}_i. \tag{14}$$

In summary, the displacement field of an element in SDST can be constructed as,

$$u(s, t) = \sum_{i=1}^{i_p} P_i(t, s)\mathbf{B}^i_{m_1}(s)\mathbf{u}_i, \qquad v(s, t) = \sum_{i=1}^{i_p} P_i(t, s)\mathbf{B}^i_{m_2}(s)\mathbf{v}_i, \tag{15, 16}$$

$$w(s, t) = \sum_{i=1}^{i_p} P_i(t, s)\mathbf{B}^i_{m_3}(s)\mathbf{w}_i, \qquad \psi_t(s, t) = \sum_{i=1}^{i_p} P_i(t, s)\mathbf{B}^i_{m_4}(s)\psi_{t_i}, \tag{17, 18}$$

$$\psi_s(s, t) = \sum_{i=1}^{i_p} P_i(t, s)\mathbf{B}^i_{m_5}(s)\psi_{s_i}, \tag{19}$$

where m_1, m_2, m_3, m_4 and m_5 are the degrees of the basis spline functions used for interpolating u, v, w, ψ_t and ψ_s, respectively. And the displacement field of an element in TST are expressed by equations (14), (15) and (16).

3. CHARACTERISTIC MATRICES OF A SDST ELEMENT

3.1. CONSTITUTIVE EQUATIONS

Within the context of first order SDST the linear constitutive equations for an arbitrary laminate are,

$$\mathbf{F} = \mathbf{L}\mathbf{e}. \tag{20}$$

where

$$\mathbf{F} = [N_s, N_t, N_{st}, M_s, M_t, M_{st}, Q_t, Q_s]^{\mathrm{T}}, \tag{21}$$

$$\mathbf{L} = \begin{bmatrix} A_{11} & A_{12} & A_{16} & B_{11} & B_{12} & B_{16} & 0 & 0 \\ & A_{22} & A_{26} & B_{21} & B_{22} & B_{26} & 0 & 0 \\ & & A_{66} & B_{61} & B_{62} & B_{66} & 0 & 0 \\ & & & D_{11} & D_{12} & D_{16} & 0 & 0 \\ & & & & D_{22} & D_{26} & 0 & 0 \\ & \text{Sym.} & & & & D_{66} & 0 & 0 \\ & & & & & & A_{44} & A_{45} \\ & & & & & & & A_{55} \end{bmatrix}, \tag{22}$$

$$\mathbf{e} = \begin{bmatrix} \partial u/\partial s + w/R_s \\ \partial v/\partial t + w/R_t \\ \partial u/\partial t + \partial v/\partial s \\ \partial \psi_s/\partial s \\ \partial \psi_t/\partial t \\ \partial \psi_s/\partial t + \partial \psi_t/\partial s + \frac{1}{2}(1/R_t - 1/R_s)(\partial v/\partial s - \partial u/\partial t) \\ \partial w/\partial t + \psi_t - v/R_t \\ \partial w/\partial s + \psi_s - u/R_s \end{bmatrix}. \tag{23}$$

The laminate stiffness coefficients in equation (22) are defined in the standard way [5, 6]. The explicit expressions for the strain vector **e** in the specified values of the displacement field can be obtained as follows using equations (15)–(19).

$$\mathbf{e} = \sum_{i=1}^{i_p} \Phi_i \, \mathbf{d}_i, \tag{24}$$

where

$$\mathbf{d}_i = [\mathbf{u}_i^{\mathrm{T}}, \mathbf{v}_i^{\mathrm{T}}, \mathbf{w}_i^{\mathrm{T}}, \psi_{t_i}^{\mathrm{T}}, \psi_{s_i}^{\mathrm{T}}]^{\mathrm{T}}, \tag{25}$$

and

$$\Phi_i = \begin{bmatrix} P_i \, \mathbf{B}_{m_1}^{i\prime} & 0 & (1/R_s)P_i \, \mathbf{B}_{m_3}^i & 0 & 0 \\ 0 & P_i' \, \mathbf{B}_{m_2}^i & (1/R_t)P_i \, \mathbf{B}_{m_3}^i & 0 & 0 \\ P_i' \, \mathbf{B}_{m_1}^i & P_i \, \mathbf{B}_{m_2}^{i\prime} & 0 & 0 & 0 \\ 0 & 0 & 0 & 0 & 0 \\ 0 & 0 & 0 & P_i' \, \mathbf{B}_{m_4}^i & 0 \\ \frac{1}{2}(1/R_s - 1/R_t)P_i' \, \mathbf{B}_{m_1}^i & \frac{1}{2}(1/R_t - 1/R_s)P_i \, \mathbf{B}_{m_2}^{i\prime} & 0 & P_i \, \mathbf{B}_{m_4}^{i\prime} & P_i' \, \mathbf{B}_{m_5}^i \\ 0 & -(1/R_t)P_i \, \mathbf{B}_{m_2}^i & P_i' \, \mathbf{B}_{m_3}^i & P_i \, \mathbf{B}_{m_4}^i & 0 \\ -(1/R_s)P_i \, \mathbf{B}_{m_1}^i & 0 & P_i \, \mathbf{B}_{m_3}^{i\prime} & 0 & P_i \, \mathbf{B}_{m_5}^i \end{bmatrix}. \tag{26}$$

3.2. STIFFNESS MATRIX

The strain energy of an element is,

$$U = \tfrac{1}{2}\int_0^A \int_{-b(s)/2}^{b(s)/2} \mathbf{e}^{\mathrm{T}}\mathbf{L}\mathbf{e}\,\mathrm{d}t\,\mathrm{d}s. \tag{27}$$

Its quadratic form in the specified values of the displacement field follows after substituting equation (24) into equation (27).

$$U = \tfrac{1}{2}\int_0^A \int_{-b(s)/2}^{b(s)/2} \sum_{i=1}^{i_p}\sum_{j=1}^{i_p} \mathbf{d}_i^{\mathrm{T}}\,\boldsymbol{\Phi}_i^{\mathrm{T}}\,\mathbf{L}\boldsymbol{\Phi}_j\,\mathbf{d}_j\,\mathrm{d}t\,\mathrm{d}s = \tfrac{1}{2}\,\mathbf{d}^{\mathrm{T}}\mathbf{k}\mathbf{d}, \tag{28}$$

where

$$\mathbf{d} = [\mathbf{d}_1^{\mathrm{T}}, \mathbf{d}_2^{T}, \ldots, \mathbf{d}_{i_p}^{\mathrm{T}}]^{\mathrm{T}}, \qquad \mathbf{k} = [\mathbf{k}_{ij}], \tag{29, 30}$$

with

$$\mathbf{k}_{ij} = \int_0^A \int_{-b(s)/2}^{b(s)/2} \boldsymbol{\Phi}_i^{\mathrm{T}}\,\mathbf{L}\boldsymbol{\Phi}_j\,\mathrm{d}t\,\mathrm{d}s. \tag{31}$$

Matrix $\mathbf{k}$ is the stiffness matrix of the element.

3.3. MASS MATRIX

When the structure undergoes harmonic motion with the amplitudes of u, v, w, ψ_t and ψ_s and natural frequency ω, the maximum kinetic energy in an element is,

$$T_{\max} = \tfrac{1}{2}\,\omega^2 \int_0^A \int_{-b(s)/2}^{b(s)/2} \mathbf{a}^{\mathrm{T}}\mathbf{H}\mathbf{a}\,\mathrm{d}t\,\mathrm{d}s, \tag{32}$$

where

$$\mathbf{a} = [u, v, w, \psi_t, \psi_s]^{\mathrm{T}}, \qquad \mathbf{H} = h\rho \begin{bmatrix} 1 & & & & \\ & 1 & & & \\ & & 1 & & \\ & & & h^2/12 & \\ & & & & h^2/12 \end{bmatrix}. \tag{33, 34}$$

The explicit expression for $\mathbf{a}$ in the specified values of the displacement field can be obtained as follows using equations (15)–(19),

$$\mathbf{a} = \sum_{i=1}^{i_p} \Gamma_i\,\mathbf{d}_i, \tag{35}$$

where

$$\Gamma_i = \begin{bmatrix} P_i\,\mathbf{B}_{m_1}^i & & & & \\ & P_i\,\mathbf{B}_{m_2}^i & & & \\ & & P_i\,\mathbf{B}_{m_3}^i & & \\ & & & P_i\,\mathbf{B}_{m_4}^i & \\ & & & & P_i\,\mathbf{B}_{m_5}^i \end{bmatrix}. \tag{36}$$

To obtain the quadratic form for the maximum kinetic energy in the specified values of the displacement field, substitute equation (35) into equation (32) to give,

$$T_{max} = \tfrac{1}{2}\,\omega^2 \int_0^A \int_{-b(s)/2}^{b(s)/2} \sum_{i=1}^{i_p} \sum_{j=1}^{i_p} \mathbf{d}_i^{\mathrm{T}}\, \Gamma_i^{\mathrm{T}}\, \mathbf{H} \Gamma_{\mathrm{j}}\, \mathbf{d}_j\, \mathrm{d}t\, \mathrm{d}s = \tfrac{1}{2}\,\omega^2 \mathbf{d}^{\mathrm{T}} \mathbf{m} \mathbf{d}, \tag{37}$$

where

$$\mathbf{m} = [\mathbf{m}_{ij}], \tag{38}$$

with

$$\mathbf{m}_{ij} = \int_0^A \int_{-b(s)/2}^{b(s)/2} \Gamma_i^{\mathrm{T}}\, \mathbf{H} \Gamma_j\, \mathrm{d}t\, \mathrm{d}s. \tag{39}$$

Matrix **m** is the mass matrix of the element.

4. CHARACTERISTIC MATRICES OF A TST ELEMENT

4.1. CONSTITUTIVE EQUATIONS

They can again be expressed by matrix equation (20). But the definitions of **F**, **L** and **e** change to,

$$\mathbf{F} = [N_s, N_t, N_{st}, M_s, M_t, M_{st}]^{\mathrm{T}}, \qquad \mathbf{L} = \begin{bmatrix} A_{11} & A_{12} & A_{16} & B_{11} & B_{12} & B_{16} \\ & A_{22} & A_{26} & B_{21} & B_{22} & B_{26} \\ & & A_{66} & B_{61} & B_{62} & B_{66} \\ & & & D_{11} & D_{12} & D_{16} \\ & \text{Sym.} & & & D_{22} & D_{26} \\ & & & & & D_{66} \end{bmatrix}, \tag{40, 41}$$

$$\mathbf{e} = \begin{bmatrix} \partial u/\partial s + w/R_s \\ \partial v/\partial t + w/R_t \\ \partial u/\partial t + \partial v/\partial s \\ -\partial^2 w/\partial s^2 + (1/R_s)\,\partial u/\partial s \\ -\partial^2 w/\partial t^2 + (1/R_t)\,\partial v/\partial t \\ -2\,\partial^2 w/\partial s\,\partial t - \tfrac{1}{2}(3/R_t - 1/R_s)\,\partial v/\partial s - \tfrac{1}{2}(3/R_s - 1/R_t)\,\partial u/\partial t \end{bmatrix}. \tag{42}$$

Substituting equations (14), (15) and (16) into equation (42) gives the explicit expression for **e** in the specified values of the displacement field.

$$\mathbf{e} = \sum_{i=1}^{i_p} \Phi_i\, \mathbf{d}_i, \tag{43}$$

where

$$\mathbf{d}_i = [\mathbf{u}_i^{\mathrm{T}}, \mathbf{v}_i^{\mathrm{T}}, \mathbf{w}_i^{\mathrm{T}}]^{\mathrm{T}}, \tag{44}$$

and

$$\Phi_i = \begin{bmatrix} P_i\,\mathbf{B}^{i'}_{m_1} & 0 & (1/R_s)N_{iH}\,\mathbf{B}^{i}_{m_3} \\ 0 & P'_i\,\mathbf{B}^{i}_{m_2} & (1/R_t)N_{iH}\,\mathbf{B}^{i}_{m_3} \\ P'_i\,\mathbf{B}^{i}_{m_1} & P_i\,\mathbf{B}^{i'}_{m_2} & 0 \\ (1/R_s)P_i\,\mathbf{B}^{i'}_{m_1} & 0 & -P_{iH}\,\mathbf{B}^{i''}_{m_3} \\ 0 & (1/R_t)P'_i\,\mathbf{B}^{i}_{m_2} & -P''_{iH}\,\mathbf{B}^{i}_{m_3} \\ \frac{1}{2}(3/R_s - 1/R_t)P'_t\,\mathbf{B}^{i}_{m_1} & \frac{1}{2}(3/R_t - 1/R_s)P_i\,\mathbf{B}^{i'}_{m_2} & -2P'_{iH}\,\mathbf{B}^{i'}_{m_3} \end{bmatrix}. \tag{45}$$

4.2. STIFFNESS MATRIX

The stiffness matrix has the same expression as equations (30) and (31) in which the definitions of Φ_i and $\mathbf{L}$ have changed to equations (45) and (41).

4.3. MASS MATRIX

The mass matrix has the same expression as equations (38) and (39). However, Γ_i and $\mathbf{H}$ in these two equations should be modified to,

$$\Gamma_i = \begin{bmatrix} P_i\,\mathbf{B}^{i}_{m_1} & & \\ & P_i\,\mathbf{B}^{i}_{m_2} & \\ & & P_{iH}\,\mathbf{B}^{i}_{m_3} \end{bmatrix}, \qquad \mathbf{H} = h\rho \begin{bmatrix} 1 & & \\ & 1 & \\ & & 1 \end{bmatrix}. \tag{46, 47}$$

5. ASSEMBLING STRUCTURAL PSEUDO STIFFNESS MATRIX AND SOLUTION PROCEDURE

Structural free vibration analysis generally requires to solve an eigenvalue problem as follows:

$$(\mathbf{K} - \lambda\mathbf{M})\mathbf{D} = 0. \tag{48}$$

The structural stiffness matrix $\mathbf{K}$ and mass matrix $\mathbf{M}$ in equation (48) can be assembled in the standard, direct fashion with those of the basic elements. Equation (48) constitutes a standard linear eigenvalue problem which could be solved using any of a wide variety methods. However, as all degrees of freedom of the structure are retained in the final set of equations and often the number is very large, most of those methods become inefficient. A way to alleviate this difficulty is by using a substructuring technique. This technique is very popular in static structural analysis. In structural vibration analysis, Wittrick and Williams [3] and Gupta [4] developed an algorithm for eigenvalue finding which can incorporate the substructuring technique naturally. This algorithm evaluates the sign count of the so called pseudo-stiffness matrix $\mathbf{S}(\lambda) = \mathbf{K} - \lambda\mathbf{M}$ to determine the positions of the required eigenvalues rather than to calculate them directly.

In the present approach the first level of substructuring involves treating each basic element as a substructure and eliminating freedoms at the internal reference meridians of each element. The second level of substructuring involves sequential doubling the identical basic element by taking advantage of the symmetric property of the shell of revolution so as to create a panel. This is an effective way to eliminate the internal freedoms of the panel. The third level of substructuring involves assembling substructures with the panels. The final level of substructuring involves a breakdown of a shell of revolution into several substructures.

Denote $\mathbf{S}(\lambda)_{i,element} = \mathbf{k}_{i,element} - \lambda \mathbf{m}_{i,element}$ as the pseudostiffness matrix of the ith basic element. Now partition $\mathbf{S}(\lambda)_{i,element}$ into the form,

$$\mathbf{S}(\lambda)_{i,element} = \begin{bmatrix} \mathbf{S}(\lambda)^{(II)}_{i,element} & \mathbf{S}(\lambda)^{(IO)}_{i,element} \\ \mathbf{S}(\lambda)^{(OI)}_{i,element} & \mathbf{S}(\lambda)^{(OO)}_{i,element} \end{bmatrix}, \tag{49}$$

in which $\mathbf{S}(\lambda)^{(II)}_{i,element}$ and $\mathbf{S}(\lambda)^{(OO)}_{i,element}$ are associated with the internal and external degrees of freedom on the internal and external reference meridians of the element. Eliminating the internal degrees of freedom obtains the pseudo-stiffness matrix of the element which is solely associated with the external degrees of freedom of the element. Its expression is as follows:

$$\mathbf{S}(\lambda)^{(OO)}_{i,element} - \mathbf{S}(\lambda)^{(OI)}_{i,element}\, \mathbf{S}(\lambda)^{(II)^{-1}}_{i,element}\, \mathbf{S}(\lambda)^{(IO)}_{i,element}. \tag{50}$$

The local boundary conditions on the internal reference meridians should be taken into account in the above eliminating process. The existing sign count $s(\lambda)_{i,element}$ for this basic element is,

$$s(\lambda)_{i,element} = s(\mathbf{S}(\lambda)^{(II)}_{i,element}), \tag{51}$$

with its right side denoting the sign count of the matrix $\mathbf{S}(\lambda)^{(II)}_{i,element}$ which can be obtained by reducing it to a triangular form that is further used to calculate equation (50).

Then, denote $\mathbf{S}(\lambda)^{1}_{j,panel}$ as the pseudostiffness matrix of the jth panel at the first doubling step, which is assembled from two identical basic element whose pseudostiffness matrices are only associated with their external degrees of freedom. Adding appropriate boundary conditions on the internal degrees of freedom of this panel and eliminating them in the same way as explained before, the obtained pseudostiffness matrix which is only associated with the external degrees of freedom of the panel at the present step is denoted as $\mathbf{S}(\lambda)^{(OO),1}_{j,panel}$ and the resulting sign count of it is $s(\lambda)^{1}_{j,panel}$. Repeating this doubling process several times (say c_j times), the obtained pseudostiffness matrix of this panel which is only associated with its external degrees of freedom is denoted as $\mathbf{S}(\lambda)^{(OO)}_{j,panel}$ and its sign count is,

$$s(\lambda)_{j,panel} = \sum_{k=0}^{c_j} 2^{c_j - k} s(\lambda)^{k}_{j,panel}, \tag{52}$$

with $s(\lambda)^{0}_{j,panel} = s(\lambda)_{i,element}$ (suppose the ith basic element is used to form the jth panel).

Next, assemble the pseudostiffness matrix of the lth substructure from those of its composed panels. In this process, rotation and eccentricity transformations about the panels may be involved. Also, appropriate boundary conditions need to be added on the internal degrees of freedom of the substructure which will be further eliminated. After this, the pseudostiffness matrix of the lth substructure which is only associated with its external degrees of freedom can be obtained and denoted as $\mathbf{S}(\lambda)_{l,sub}$. The existing sign count of this substructure is,

$$s(\lambda)_{l,sub} = s(\mathbf{S}(\lambda)^{(II)}_{l,sub}) + \sum_{j=1}^{J_l} s(\lambda)_{lj,panel}, \tag{53}$$

where the first term in the right side of the above equation is the sign count of the pseudostiffness matrix of this substructure which is only associated with its internal degrees of freedom. J_l is the number of panels in it.

Finally, assemble the pseudo-stiffness matrix $\mathbf{S}(\lambda)_{top}$ of the entire structure from those of its composed substructures. In this process, the rotation transformation about the substructures may be used. Using Gauss elimination procedure to reduce the

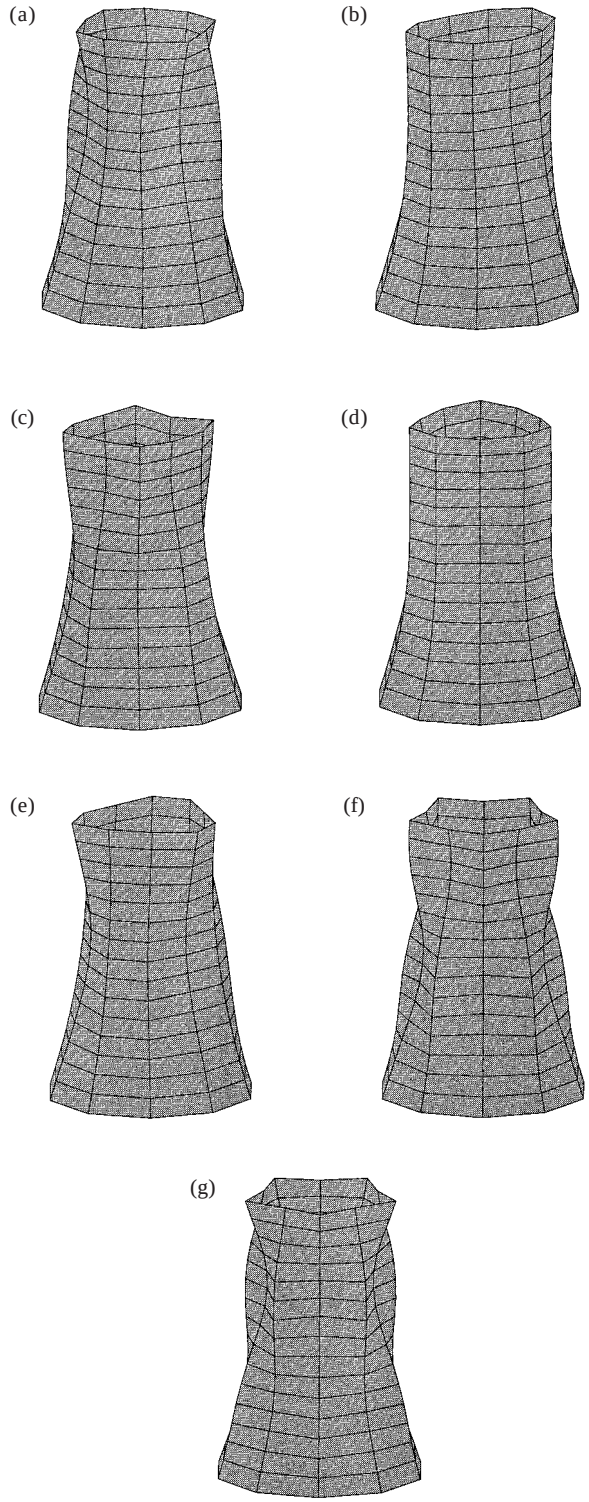

Figure 2. Mode shapes of a cooling tower calculated with a coarse mesh: (a) first mode ($m = 1, n = 4$); (b) second mode ($m = 1, n = 3$); (c) third mode ($m = 1, n = 6$); (d) fourth mode ($m = 1, n = 2$); (e) fifth mode ($m = 2, n = 3$); (f) sixth mode ($m = 2, n = 5$); (g) seventh mode ($m = 3, n = 5$).

pseudostiffness matrix of the top level structure after having applied boundary conditions to the appropriate degrees of freedom of it, its sign count can be found and denoted as $s(\lambda)_{top}$. Therefore, the sign count of the entire structural pseudostiffness matrix calculated in the multi-level substructuring way is,

$$s(\lambda)_{struc} = s(\lambda)_{top} + \sum_{l=1}^{J} s(\lambda)_{l,sub}. \tag{54}$$

The quantity $s(\lambda)_{struc}$ provides the basis for the determination of eigenvalues, since knowledge of its value indicates with certainty how many eigenvalues lie below any chosen value of λ. It is quite simple to use this property to establish upper and lower bounds to any required eigenvalue. Having done this, there are a number of possible iteration procedures which converge the required eigenvalue with a specified level of accuracy. In the present work a simple Golden section method is used.

Once a required eigenvalue is determined it may be desired to find the corresponding eigenvector. To this end, the following equation must be solved first,

$$\mathbf{S}(\lambda^*)_{top}\,\mathbf{D}_{top} = \mathbf{Q}, \tag{55}$$

where λ^* is the calculated eigenvalue. $\mathbf{D}_{top}$ is the eigenvector associating with the degrees of freedom retained at the top structural level. Column vector $\mathbf{Q}$ needs to be specified. Quite commonly all terms of $\mathbf{Q}$ are taken to be zero except for the last term, which is assigned an arbitrary value. However, this procedure has been shown to be inaccurate and a detailed study [8] has revealed that the most reliable method of determining $\mathbf{D}_{top}$ via equation (55) is to assign a random value to each term of $\mathbf{Q}$. This is the method that has been used in the present study.

After $\mathbf{D}_{top}$ has been calculated, the elements of the eigenvector which are associated with the internal degrees of freedom at different levels of substructuring can be found using a general equation as follows,

$$\mathbf{D}_I = -\mathbf{S}(\lambda^*)^{(II)^{-1}}\mathbf{S}(\lambda^*)^{(IO)}\mathbf{D}_O, \tag{56}$$

TABLE 1

Natural frequencies (Hz) *of a circular cylinder* ($m = 1$). *The upper and lower values are from TST and SDST analysis, respectively.*

Number of elements	Circumferential number (n)					
	7	6	8	9	5	10
16*	418·8	425·0	455·7	502·4	706·4	747·3
	418·8	424·9	455·6	502·4	706·4	746·5
32	383·5	401·1	422·5	497·7	498·9	600·8
	383·4	401·1	422·4	497·7	498·8	600·6
64	380·8	400·1	416·9	488·9	497·5	584·4
	380·7	400·1	416·8	488·8	497·5	584·3
256	380·7	400·1	416·7	488·6	497·5	583·9
	380·7	400·1	416·7	488·5	497·5	583·8
Flugge's theory [9]	380·7	400·1	416·7	488·6	497·5	583·9

* Note: the natural frequencies are listed in a numerically ascending order which do not necessarily correspond with the circumferential numbers shown above them as the coarse mesh used in this case)

where $\mathbf{D}_O$ is a vector containing the elements of the eigenvector which are associated with the external degrees of freedom at corresponding levels of substructuring. Principally, the above process for calculating the elements of eigenvectors can be carried out to any level of substructure provided that the relationships of the substructures at various levels are stored during the calculation. In the present study, the above process retreats to the level of panels.

6. APPLICATIONS

The proposed method in the context of SDST and TST has been programmed. Selected free vibration applications involving the use of this integrated software are described in what follows. In all applications, the basic elements run the full length of a shell of revolution and four reference meridians are used (i.e., $i_p = 4$) in every basic element, and the degree of spline functions for interpolating u, v, w and ψ_t is 3 (i.e., $m_1 = m_2 = m_3 = m_4 = 3$) and that for ψ_s is 2 (i.e. $m_5 = 2$).

6.1. FREE VIBRATION OF A CIRCULAR CYLINDER

The length, radius and thickness of this circular cylinder are 298·20 mm, 148·23 mm 0·508 mm, respectively. Its material properties are Younge's modulus $E = 203{\cdot}44\ \text{kN/mm}^2$, Poisson ratio $v = 0{\cdot}285$ and density $\rho = 7{\cdot}8459 \times 10^{-6}\ \text{kg/mm}^3$. It has diaphragm ends. Five nodes are evenly distributed along the meridian. Both TST and SDST analysis are employed. The calculated results for the first six natural frequencies using different number of elements circumferentially are recorded in Table 1. For comparison, the theoretical results by Egle and Soder [9] using Flugge's thin shell theory are also given in Table 1.

The above results show that on one hand the present method can quickly converge to the exact solution and on the other hand the coarse mesh (the case using 16 elements) can greatly distort the results.

6.2. FREE VIBRATION OF A COOLING TOWER

This example is from reference [10]. The cooling tower is an elliptic hyperboloid shell of uniform thickness of 0·13 m. Its height is 95·25 m. Its radius at the bottom and top are

TABLE 2

Natural frequencies (Hz) *of a cooling tower calculated with a coarse mesh*. (*The values in parentheses are from* [10].)

	Circumferential number (n)					
Meridional number (m)	1	2	3	4	5	6
1	4·251	2·016	1·631	1·561	3·490	1·755
	(4·002)	(2·121)	(1·684)	(1·577)	(3·498)	(1·885)
	–	–	–	4·407	–	–
	–	–	–	(4·483)	–	–
2	–	4·810	2·277	3·238	2·846	3·788
	–	(4·613)	(2·465)	(3·208)	(2·723)	(3·956)
	–	–	–	3·644	–	–
	–	–	–	(3·630)	–	–
3	–	–	–	4·373	3·021	–
				(4·321)	(3·104)	–

TABLE 3

Natural frequencies (Hz) *of a cooling tower calculated with refined meshes using TST analysis*. (*The values in parentheses correspond to the mesh with* 64 *elements*.)

	Circumferential number (n)						
Meridional number (m)	2	3	4	5	6	7	8
1	2·015	2·267	1·652	–	–	–	–
	(2·015)	(2·267)	(1·652)	–	–	–	–
2	–	1·611	1·477	1·428	1·723	–	–
	–	(1·611)	(1·477)	(1·426)	(1·708)	–	–
3	–	–	–	1·677	1·768	2·070	2·490
	–	–	–	(1·675)	(1·764)	(2·060)	(2·475)
	–	–	–	2·610	2·595	2·182	
	–	–	–	(2·609)	(2·593)	(2·172)	
4	–	–	–	–	–	–	2·656
	–	–	–	–	–	–	(2·654)

36·85 m and 24·02 m, respectively, and that at height of 76·81 m is 22·99 m. The meridian of the cooling tower is a parabola. The bottom is fixed and the top is free. The material is assumed to be isotropic having Young's modulus $E = 29{\cdot}60\ \mathrm{GN/m^2}$, Poisson ratio $\nu = 0{\cdot}15$ and density $\rho = 2400\ \mathrm{kg/m^3}$. In reference [10], Yang and Kapania calculated the first fifteen natural frequencies using 48 dof quadrilateral doubly curved shell element with a 5×5 mesh for half the shell. For comparison, six nodes evenly distributed along the meridian and ten elements are used in the present method which is equivalent to the mesh division used by Yang and Kapania. The results from both methods using TST analysis are recorded in Table 2, and some of the mode shapes calculated using the present method are shown in Figure 2.

The two results seem to be very close to each other. But from the obtained mode shapes in Figure 2, it is seen that the mesh is too coarse. So two refined meshes are used which have 32 and 64 elements respectively with eleven evenly distributed nodes on the meridian. The obtained natural frequencies using both TST and SDST analysis are recorded in Tables 3 and 4 and the first seven mode shapes (they are same for both refined meshes) are depicted in Figure 3.

It can be seen from Tables 2 and 3 that the natural frequencies are substantially different between the results from the coarse mesh and the refined meshes. The reason may be that the shell is a sensitive structure and the mesh division will greatly affect the final results. From Figures 2 and 3, it is also seen that the meridional number and the circumferential number of the mode shapes can be perceived easier in the refined meshes than in the coarse one. From Tables 3 and 4 it is seen that the obtained natural frequencies are convergent and the results between TST and SDST analysis are quite close because the shell is effectively thin.

To do more exercises with the present method and its corresponding software, the vibrational behaviours of an elliptic hyperboloid shell having the same geometry as the above but different material properties are analyzed. First, an orthotropic material property is chosen with E_L (meridional direction) $= 29{\cdot}60\ \mathrm{GN/m^2}$, E_T (circumferential direction) $= 9{\cdot}60\ \mathrm{GN/m^2}$, $G_{LT} = G_{TT} = 4{\cdot}2899\ \mathrm{GN/m^2}$, and $\nu_{LT} = 0{\cdot}15$. Then an anisotropic material is used which is obtained by just rotating the above orthotropic material an angle of 30°, i.e., the angle between the fibre direction and the meridian is 30°. Their

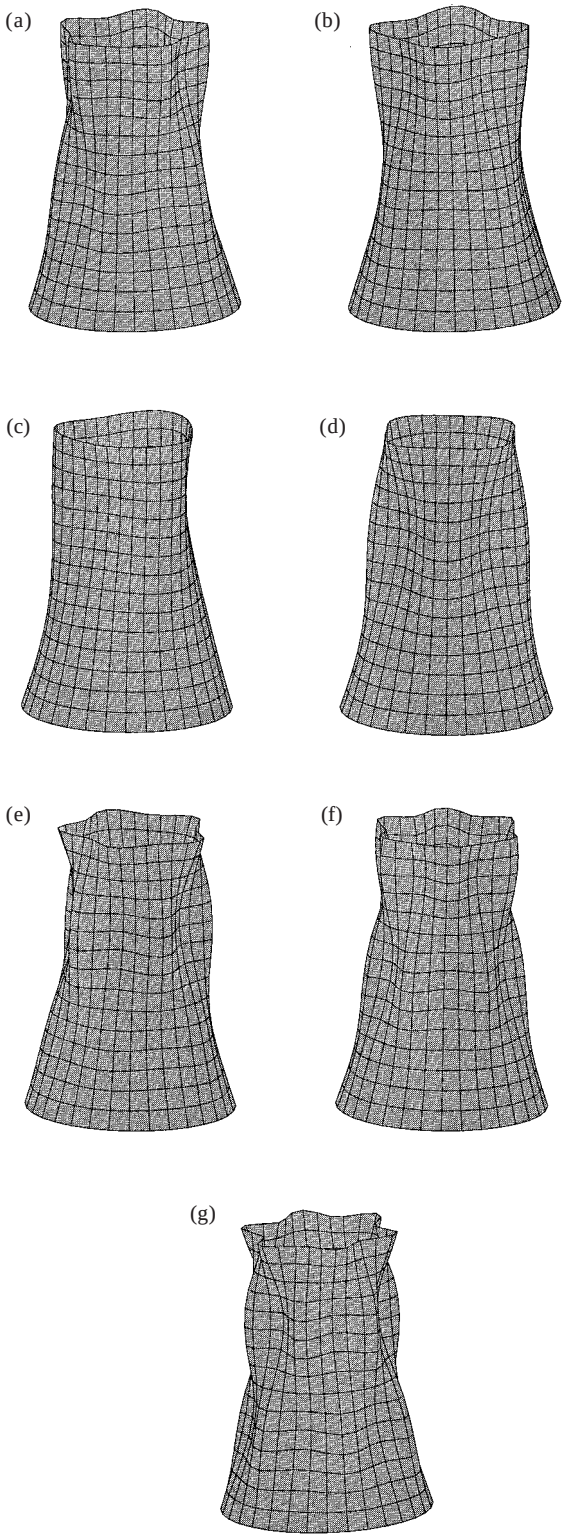

Figure 3. Mode shapes of a cooling tower calculated with refined meshes: (a) first mode ($m = 2, n = 5$); (b) second mode ($m = 2, n = 4$); (c) third mode ($m = 2, n = 3$); (d) fourth mode ($m = 1, n = 4$); (e) fifth mode ($m = 3, n = 5$); (f) sixth mode ($m = 2, n = 6$); (g) seventh mode ($m = 3, n = 6$).

TABLE 4

Natural frequencies (Hz) *of a cooling tower calculated with refined meshes using SDST analysis*. (*The values in parentheses correspond to the mesh with* 64 *elements*.)

	Circumferential number (n)						
Meridional number (m)	2	3	4	5	6	7	8
1	2·014	2·265	1·648	–	–	–	–
	(2·014)	(2·265)	(1·647)	–	–	–	–
2	–	1·607	1·477	1·427	1·712	–	–
	–	(1·607)	(1·477)	(1·425)	(1·707)	–	–
3	–	–	–	1·675	1·768	2·070	2·490
	–	–	–	(1·673)	(1·764)	(2·060)	(2·474)
	–	–	–	2·610	2·595	2·182	–
	–	–	–	(2·609)	(2·592)	(2·171)	–
4	–	–	–	–	–	–	2·656
	–	–	–	–	–	–	(2·637)

TABLE 5

Natural frequencies (Hz) *of an orthotropic elliptic hyperboloid shell*. (*The values in parentheses correspond to the mesh with* 64 *elements*.)

		Circumferential number (n)		
Meridional number (m)	Theory	4	5	6
2	TST	1·124	1·065	1·151
		(1·122)	(1·064)	(1·151)
	SDST	1·122	1·062	1·150
		(1·119)	(1·061)	(1·150)
3	TST	–	1·208	1·218
		–	(1·208)	(1·216)
	SDST	–	1·205	1·217
		–	(1·204)	(1·214)

TABLE 6

Natural frequencies (Hz) *of an anisotropic elliptic hyperboloid shell*. (*The values in parentheses correspond to the mesh with* 64 *elements*.)

		Circumferential number (n)			
Meridional number (m)	Theory	3	4	5	6
2	TST	1·093	0·972	0·981	1·174
		(1·093)	(0·971)	(0·980)	(1·171)
	SDST	1·088	0·968	0·978	1·173
		(1·088)	(0·968)	(0·977)	(1·170)
3	TST	–	–	1·245	–
		–	–	(1·243)	–
	SDST	–	–	1·244	–
	–	–	–	(1·241)	–

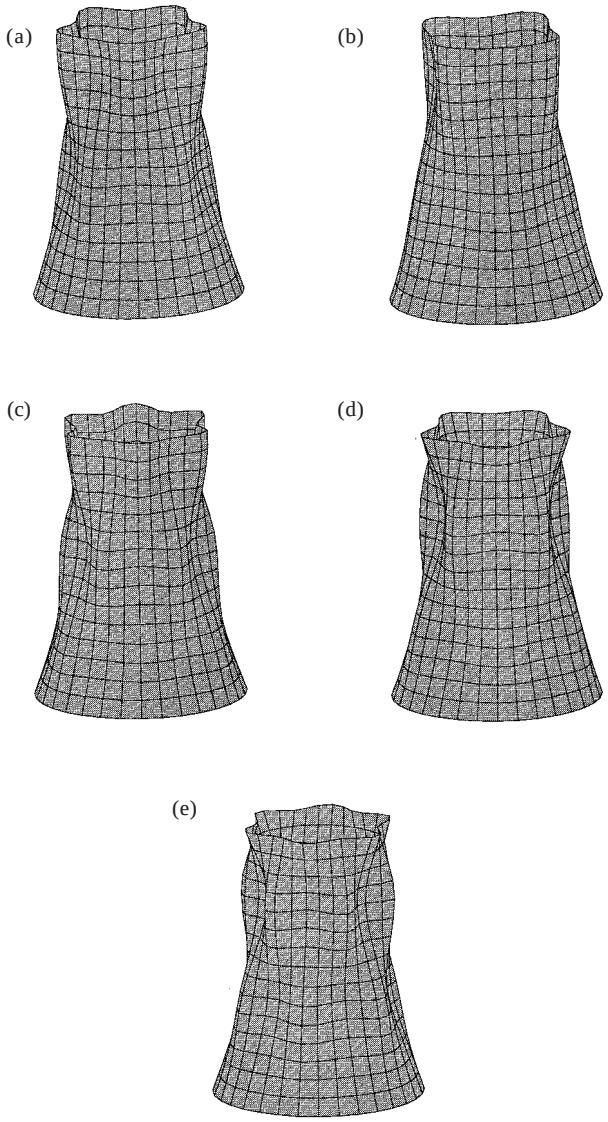

Figure 4. Mode shapes of an orthotropic elliptic hyperboloid shell: (a) first mode ($m = 2$, $n = 5$); (b) second mode ($m = 2$, $n = 4$); (c) third mode ($m = 2$, $n = 6$); (d) fourth mode ($m = 3$, $n = 5$); (e) fifth mode ($m = 3$, $n = 6$).

first five natural frequencies and the corresponding mode shapes are calculated. The results are recorded in Tables 5 and 6 and shown in Figures 4 and 5 (mode shapes are same for both meshes), respectively.

The values in Tables 5 and 6 indicate that the calculated natural frequencies are convergent and the results between TST and SDST analysis are again very close. It is not surprising to see that the mode shapes in Figure 5 are highly skewed because of the anisotropic material used in this case.

6.3. FREE VIBRATION OF A COMPLETE SPHERICAL SHELL

The radius and thickness of the spherical shell are 36·85 m and 0·13 m, respectively. The isotropic material properties for the spherical shell are the same as in the above example.

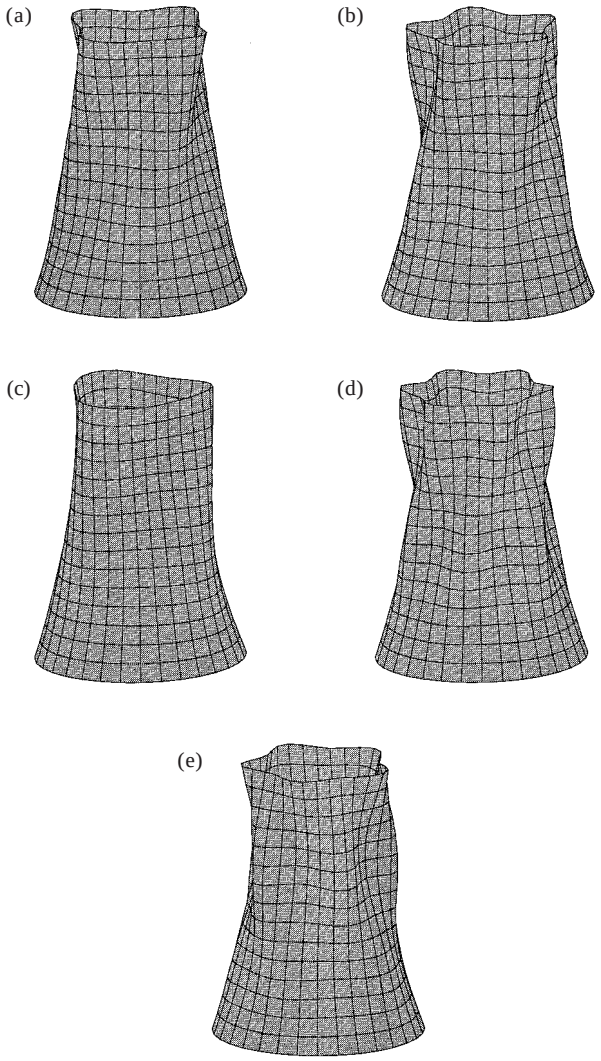

Figure 5. Mode shapes of an anisotropic elliptic hyperboloid shell: (a) first mode ($m = 2, n = 4$); (b) second mode ($m = 2, n = 5$); (c) third mode ($m = 2, n = 3$); (d) fourth mode ($m = 2, n = 6$); (e) fifth mode ($m = 3, n = 5$).

TABLE 7

Natural frequencies (Hz) *of a complete spherical shell*. (*The values in parentheses are corresponding to the mesh with* 64 *elements*.)

	Mode						
Theory	1	2	3	4	5	6	7
TST	11·33 (11·33)	12·23 (12·23)	12·27 (12·27)	13·67 (13·67)	14·07 (14·07)	14·26 (14·26)	14·38 (14·38)
SDST	11·33 (11·32)	12·23 (12·23)	12·27 (12·27)	13·67 (13·67)	14·07 (14·07)	14·26 (14·26)	14·38 (14·38)

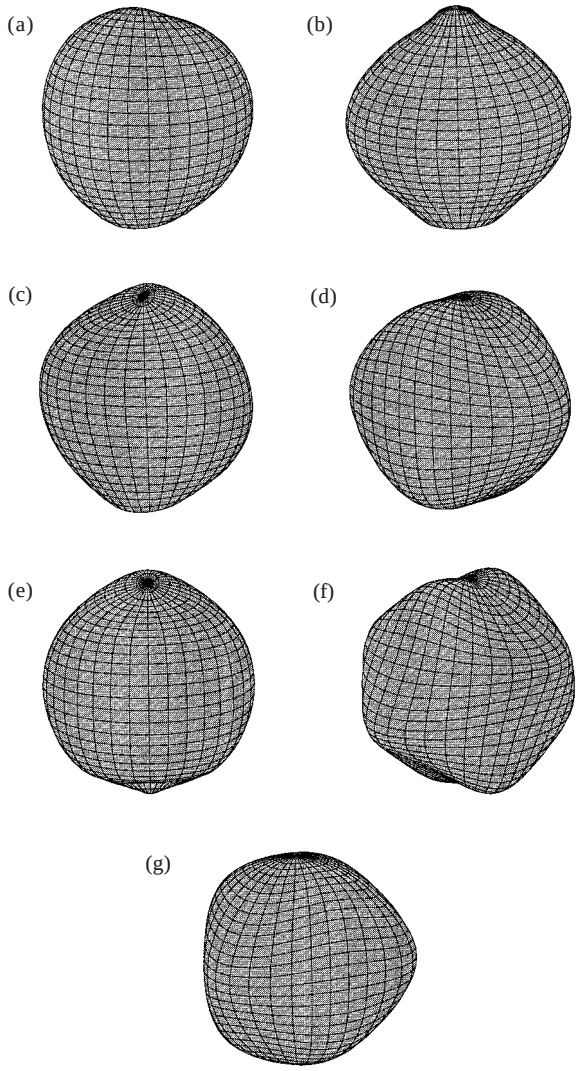

Figure 6. Mode shapes of a complete spherical shell: (a) first mode; (b) second mode; (c) third mode; (d) fourth mode; (e) fifth mode; (f) sixth mode; (g) seventh mode.

The displacements in the x, y and z directions at two poles are restrained. Eleven nodes evenly distributed along the meridian and 32 and 64 elements are again used, respectively. The first seven natural frequencies calculated using both TST and SDST analysis are recorded in Table 7 and their corresponding mode shapes (same for both meshes) are shown in Figure 6.

From Table 7 it is clear that the results are convergent and they are almost the same for the TST and SDST analyses. There is no existing solution for this demanding application. So comparison is omitted. From Figure 6, it is quite interesting to see that the mode shapes of a spherical shell have their own distinct characters which are rarely observed in other types of shells.

7. CONCLUSIONS

A very efficient numerical method for analyzing the free vibration of shells of revolution is presented. A multi-level substructuring technique is used in conjunction with the Sturm sequence method for eigenvalue finding. Both thin and thick shells of revolution with arbitrary laminations and boundary specification can be analyzed using the SDST and TST analysis capabilities of the present method. The element constructed in this method is unlike the usual elements which have fixed degrees of freedom and fixed order of continuity of the interpolated displacement field. Its degrees of freedom can be increased or decreased without changing the order of continuity of the interpolated displacement field. The applications for this method show both its validity, efficiency and accuracy and its potential use for more complicated structures involving shells of revolution which are often encountered in aerospace engineering, marine engineering, power plant engineering and civil engineering.

ACKNOWLEDGMENT

The author would like to thank the referees' helpful comments.

REFERENCES

1. H. Stolarski, T. Belytschko and S.-H. Lee 1995 *Computational Mechanics Advances* **2**, 125–212, Review of shell finite element and corotational theories.
2. O. C. Zienkiewicz and R. L. Taylor 1991 *Finite Element Method*. volume II. New York: McGraw Hill.
3. W. H. Wittrick and F. W. Williams 1971 *Quarterly Journal of Mechanics and Applied Mathematics* **24**, 263–284. A general solution for computing natural frequencies of elastic structures.
4. K. K. Gupta 1972 *International Journal of Numerical Methods in Engineering* **4**, 379–404. Solution of eigenvalue problems by Sturm sequence method.
5. J. N. Reddy 1984 *Journal of Engineering Mechanics*, ASCE **110**, 794–805. Exact solution of moderately thick laminated shells.
6. A. W. Leissa and J.-D. Chang 1996 *Composite Structures* **35**, 153–170. Elastic deformation of thick, laminated composite shells.
7. Walter Schempp 1982 *Complex Contour Integral Representation of Cardinal Spline Functions*. American Mathematical Society.
8. C. T. Hopper and F. W. Williams 1972 *Journal of Structural Mechanics* **5**, 255–278. Mode finding in nonlinear structural eigenvalue calculations.
9. D. M. Egle and K. E. Soder 1968 *Final Report* (*Part* 1) *of NASA Grant*. A theoretical analysis of the free vibration of discretely stiffened cylindrical shells with arbitrary end conditions.
10. T. Y. Yang and R. K. Kapania 1984 *Journal of Engineering Mechanics*, ASCE **110**, 589–603. Finite element random response analysis of cooling tower.